Original Research

Shock waves increase pulmonary vascular leakage, inflammation, oxidative stress, and apoptosis in a mouse model

Changci Tong, Yunen Liu, Yubiao Zhang, Peifang Cong, Xiuyun Shi, Ying Liu, Lin Shi Hongxu Jin and Mingxiao Hou

Emergency Medicine Department of General Hospital of Shenyang Military Command, Laboratory of Rescue Center of Severe Wound and Trauma PLA, Shenyang 110016, China
Corresponding author: Mingxiao Hou. Email: houmingxiao188@163.com

Impact statement

The number of patients with explosive injury has increased year by year, but there is no better treatment. However, the research on detonation injury is difficult to carry out. One of the factors is the difficulty in making the model of blast injury. The laboratory successfully developed and produced a simulation device of explosive knocking through a large amount of literature data and preliminary experiments, and verified the preparation of the simulation device through various experimental techniques. The results showed that the device could simulate the shock wave-induced acute lung injury generated, which was similar to the actual knocking injury. The experimental process was controlled. Under the same condition, there was no statistical difference between the groups. It is possible to realize miniaturization and precision of an explosive knocking simulation device, which is a good experimental tool for further research on the mechanism of organ damage caused by detonation and the development of protective drugs.

Abstract

Severe lung damage is a major cause of death in blast victims, but the mechanisms of pulmonary blast injury are not well understood. Therefore, it is important to study the injury mechanism of pulmonary blast injury. A model of lung injury induced by blast exposure was established by using a simulation blast device. The effectiveness and reproducibility of the device were investigated. Eighty mice were randomly divided into eight groups: control group and 3 h, 6 h, 12 h, 24 h, 48 h, 7 days and 14 days post blast. The explosive device induced an explosion injury model of a single lung injury in mice. The success rate of the model was as high as 90%, and the degree of lung injury was basically the same under the same pressure. Under the same conditions, the thickness of the aluminum film can be from 0.8 mm to 1.6 mm, and the peak pressure could be from 95.85 ± 15.61 PSI to 423.32 ± 11.64 PSI. There is no statistical difference in intragroup comparison. A follow-up lung injury experiment using an aluminum film thickness of 1.4 mm showed a pressure of 337.46 ± 18.30 PSI induced a mortality rate of approximately 23.2%. Compared with the control group (372 ± 23 times/min, 85.9 ± 9.4 mmHg, 4.34 ± 0.09), blast exposed mice had decreased heart rate (283 ± 21 times/min) and blood pressure (73.6 ± 3.6 mmHg), and increased lung wet/dry weight ratio(2.67 ± 0.11), marked edematous lung tissue, ruptured blood vessels, infiltrating inflammatory cells, increased NF-κB (4.13 ± 0.01), TNF-α (4.13 ± 0.01), IL-1β (2.43 ± 0.01) and IL-6 (4.65 ± 0.01) mRNA and protein, decreased IL-10(0.18 ± 0.02) mRNA and protein ($P < 0.05$). The formation of ROS and the expression of MDA5 (4.46 ± 0.01) and IREα (3.43 ± 0.00) mRNA and protein were increased and the expression of SOD-1 (0.28 ± 0.02) mRNA and protein was decreased ($P < 0.05$). Increased expression of Bax (3.54 ± 0.00) and caspase 3 (4.18 ± 0.01) mRNA and protein inhibited the expression of Bcl-2 (0.39 ± 0.02) mRNA and protein. The changes of pulmonary edema, inflammatory cell infiltration, and cell damage factor expression increased gradually with time, and reached the peak at 12–24 h after the outbreak, and returned to normal at 7–14 days. Detonation injury can lead to edema of lung tissue, pulmonary hemorrhage, rupture of pulmonary vessels, induction of early inflammatory responses accompanied by increased oxidative stress in lung tissue cells and increased apoptosis in mice experiencing blast injury. The above results are consistent with those reported in other literatures. It is showed that the mouse lung blast injury model is successfully modeled, and the device can be used for the study of pulmonary blast injury.

Keywords: Blast exposure, lung injury, inflammatory, oxidative stress, apoptosis, simulation device for lung blasting

Experimental Biology and Medicine **2018; 243: 934–944. DOI: 10.1177/1535370218784539**

Copyright © 2018 by the Society for Experimental Biology and Medicine

Introduction

In recent years, the death rate of young adults has increased due to an increase in war and terrorist activities compared with the death rate attributable to traffic accidents, high fall injuries, and occupational injuries.[1,2] The most common cause of death of those involved in an explosion is trauma to the chest.[3] Damage caused by an explosion can be divided into four types: 1, shock waves directly injuring the body such as lung blast injury; 2, debris directly impacting the body causing by damage; 3, shock waves caused by the physical displacement of the wound damage; and 4, explosion caused by chemical and thermal damage. Damage caused by shock waves is the most common in these four types of damage.[4,5]

Lung blast injury (LBI) can lead to increased intraarterial pressure, which causes immediate or delayed pulmonary bleeding and alveolar, pulmonary capillary rupture, pulmonary hemorrhage, and pulmonary edema, and further deterioration as well as acute lung injury (ALI), acute respiratory distress syndrome (ARDS), and multiple organ dysfunction syndrome (MODS), which eventually lead to death.[6,7] Bomb disabled persons manifested as hemothorax and pneumothorax, died of multiple organ failure and septic shock.[8] Therefore, it is of great importance to study the injury process of pulmonary blast injury.

Accurate and reproducible modeling is an indispensable experimental means of studying shock wave-induced lung injury. At present, the existing literature has reported the induction of pulmonary blast injury using nitrogen compression or the direct application of bomb-directed blasting shocks to cause lung injury.[9–15] However, the experimental conditions of these methods are not controllable and the result of the experiment is quite different. Furthermore, most of the existing equipment is very large and expensive and requires complex operation.

Therefore, it is necessary to be able to study the mechanism of blasting injury, using a method that makes it easy to record the experimental conditions, with a high repetition rate, simple operation, low site requirement, and low cost.

The purpose of this study was to design an explosion shock wave simulation device for pulmonary blasting and verify the damage mechanism of lung blast induced by shock wave alone in mice. We successfully developed a pulmonary blasting simulation device containing a pressure pump to simulate a shock wave generated by blasting. The use of protection device allows the control of the acute model of pulmonary blast injury. Shock waves were exposed only to the chest, while excluding shrapnel and the heat generated by an explosion that can cause damage. The experimental process has a high repetition rate, simple operation, and accurately simulates a pulmonary blast. The miniaturization and precision of the simulation device have been realized. Our results show that pulmonary blast injury can lead to pulmonary edema in mice, pulmonary vascular rupture, and induced early inflammatory response accompanied by increased oxidative stress in lung tissue cells, which increases apoptosis.

Materials and methods

Experimental animals

Eighty healthy male Kunming mice weighing 25–30 g and six to eight weeks of age were purchased from the Shenyang Military Region General Hospital Experimental Animal Center. Mice were fed and allowed access to drinking water ad libitum. Animal welfare and experimental design were approved by the Shenyang Military Region General Hospital Ethics Committee.

Design of a simulation device for lung blasting

The rock blasting shock simulation device was based on a study by Awwad *et al.*[16] which used an explosion shock model. The LBI model was induced by using compressed air to form a shock wave produced by an aluminum film directed at the chest of a mouse. The lung blasting simulation device consists of four parts: air compression device, fixture, protection device, and data acquisition device. As shown in Figure 1(a), the bottom of the device is the air compression device, a length of about 100 cm of steel pipe connected to the air pressure pump and power supply. The main device is above a 30 cm steel pipe, the top surface for the wire. The fixed protective cover contains the middle of the connection pressure sensor. The top of the main body and the lower device can be placed in the middle of different thicknesses of an aluminum film, attached by screws. The peak pressure increased by increasing the aluminum thickness, which provides different degrees of lung shock damage. The protection device consists of a hard plastic cylinder, containing a hole for mice to enter, allowing specific parts of the mouse to be exposed to the shock wave. Shock wave pressure data are obtained from the pressure sensor, and measurements are transmitted through a data cable and stored on a computer.

Preparation of mouse LBI model

Mice were anesthetized by the intraperitoneal injection of 2% pentobarbital sodium (1.5 mL/kg). The anesthetized mice were placed in a protective cover, their chest exposed, and the aluminum placed in the middle layer. The screws were fixed and the mouse placed on the wire mesh on the top of the device. The pressure pump compressed the air, increasing the air pressure in the lower device, until the aluminum film ruptured. Then the compressed air instantaneously rapidly expanded from the blasting port at high speed to form shock waves that impact the chest of the mouse. The pressure reading from the sensor is transmitted through a data cable to a computer to form a waveform using the formula: pressure (PSI) = voltage value $\times$ 1000/50.08. This converts the computer-recorded electrical signal to a pressure value (Figure 1(b)) and records the death rate of mice on the spot. After 2 h, the mice regained consciousness and acted slowly, and returned to normal after 6 h.

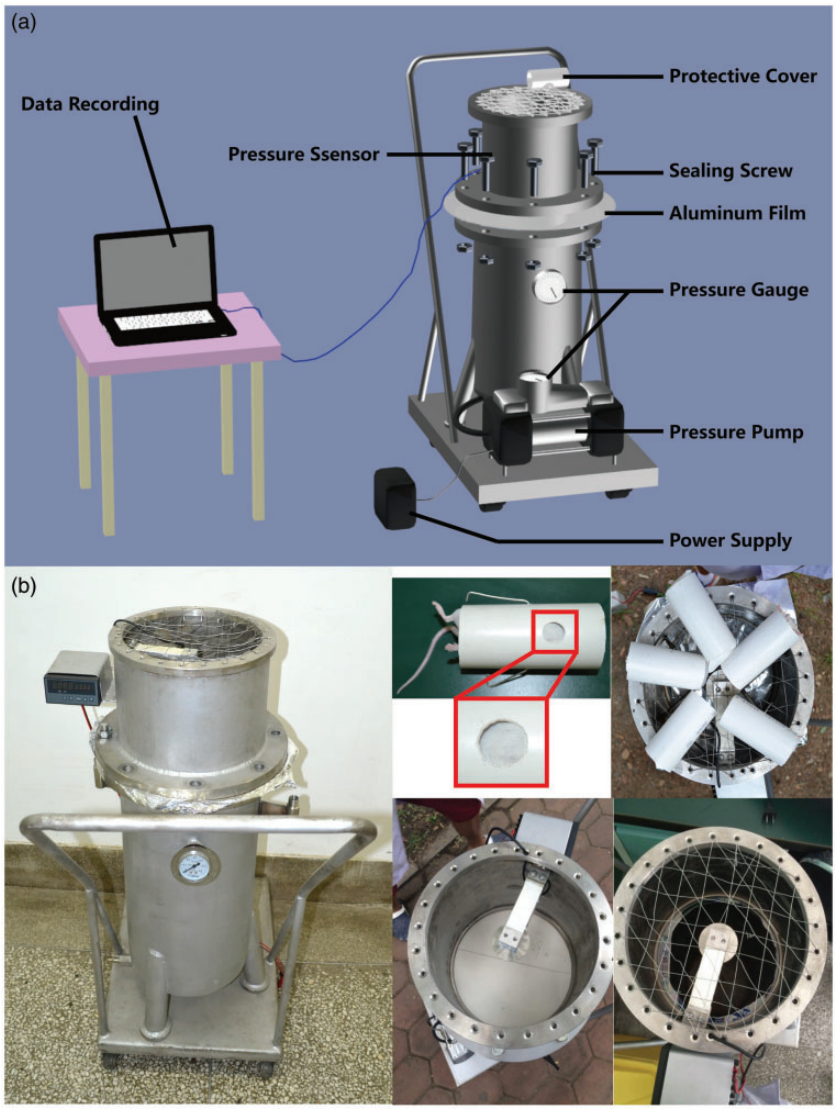

Figure 1. Design and installation of a simulated device for pulmonary blasting. (a) The main body of the device below the air compression device, including a steel pipe, air pressure pump, and power supply; a main device above the wire mesh that is a fixed protective cover; a middle connection pressure sensor. The main body can be placed in the middle of the aluminum film. When connected to the power supply, air is compressed and breaks through the aluminum film resulting in a shock wave on the mouse chest. The other parts of the mouse are under protective cover to block the shock wave. Shock wave pressure data are measured by a pressure sensor, and transmitted to a computer. (b) Pulmonary blast shock simulation device. Anesthetized mice are placed in a protective hood, and the round hole on the exposed shield of the chest is placed against the wire mesh to prevent secondary damage caused by shock waves to the ground. An accurate model of lung blast injury in five mice could be prepared at one time. (A color version of this figure is available in the online journal.)

Experimental grouping

Eighty mice were randomly divided into control groups: 3 h, 6 h, 12 h, 24 h, 48 h, 7 days and 14 days post blast. After the LBI was successfully modeled, the mice were sacrificed at different times. Eighty mice were numbered according to their body weight. Starting from any row in the random number table, 80 random numbers were recorded. In the event of the same number, the next random number was copied. The random numbers were sorted in ascending order. From the sorted number, the first 10 are defined as the first group, and so on.

Heart rate and blood pressure detection

At the end of 3 h, 6 h, 12 h, 24 h, 48 h, 7 days and 14 days post blast, the anesthetized mice of five in each group were treated with a pentobarbital intraperitoneal injection. After the left femoral artery was placed, an artery cannula, a blood pressure sensor was connected to the heart function analyzer. An electrocardiogram was used to continuously monitor the mouse heart rate and blood pressure.

Sample collection

After detecting heart rate and blood pressure, mice were fixed in a prone position to a small animal operating table. After opening the abdominal cavity, the mice were sacrificed by collecting blood through the abdominal aorta. The lungs were removed, and the left lung was placed in 10% formalin buffer. Paraffin embedding and slices were used for HE staining and histological changes were observed. The moisture content of the upper right lobe of

the right lung was blotted with filter paper, and weighed on an analytical balance. The wet weight was recorded and it was then placed in a 60°C oven for 72 h to constant weight. The dry weight was recorded and the dry weight was calculated. Tissue residues were placed directly in liquid nitrogen tanks for storage until gene and protein detection.

HE

Paraffin section was dewaxed in water, then hematoxylin-stained for 5 min, rinsed with water for 5 min, and then was incubated in 1% acetic acid ethanol for 30 s, washed, stained with 0.5% eosin for 1–3 min, washed in distilled water for 30 s after dehydration, sealed with neutral gum, and observed under a microscope.

Lung injury score

The lung injury was scored according to the HE results and pathologic scoring criteria.[16] Lung injury scores were quantified based on changes in the lung structure. Microscopic damage was scored according to the following variables: alveolar and interstitial inflammation, alveolar and interstitial hemorrhage, edema, atelectasis, and necrosis. The severity of the damage was graded as follows, with each of the seven variables: no damage was graded as 0 points, damage with 25% was 1 point, damage with 50% was 2 points, damage with 75% was 3 points, and diffuse damage was 4 min. The highest score is 28 points and the lowest is 0 points.

Detection of pulmonary vascular injury

After successful modeling, 2% Evans blue (2 mL/kg) was injected intravenously 30 min before the other five mice were sacrificed in each group. After the abdominal injection of 2% pentobarbital sodium (1.5 mL/kg) after anesthesia, the chest was opened, the right atrium was cut, and intrahepatic perfusion of heparin saline (0.9% sodium chloride + 20 U/mL heparin sodium) was performed followed by a 100 mL rinse. The lung tissue was weighed, cut, placed into 1 mL N,N-Dimethylformamide (DMF), homogenized after 60°C incubation for 24 h, and centrifuged at 12,000 r/min for 20 min. A microplate was used to detect the wavelength at 630 nm absorbance, according to the standard curve calculation of lung tissue based on Evans blue content.

Western blot

The protein samples were added to the corresponding proportion of SDS gel loading buffer, boiled and denatured for 5 min, underwent SDS-PAGE electrophoresis, transferred to 5% skim milk PBST buffer at room temperature for 1 h, and washed in PBST for three times. Then the appropriate primary antibody NF-κB (1:2000; cat. no. ab16502; Abcam, Cambridge, UK), TNF-α (1:1000; cat. no. ab8348; Abcam, Cambridge, UK), IL-1β (1:1000; cat. no. sc-7884; Santa Cruz Biotechnology, Inc., Dallas, TX, USA), IL-4 (1:1000; cat. no. sc-73318; Santa Cruz Biotechnology, Inc., Dallas, TX, USA), IL-6 (1:1000; cat. no. ab83053; Abcam, Cambridge, UK), IL-10 (1:2000; cat. no. ab9969; Abcam, Cambridge, UK), MDA5 (1:1000; cat. no. ab69983; Abcam, Cambridge, UK), IREα (1:2000; cat. no. #3294; Cell Signaling Technology, Boston, USA), SOD-1 (1:1000; cat. no. sc-11407; Santa Cruz Biotechnology, Inc., Dallas, TX, USA), Bax (1:2000; cat. no. sc-526; Santa Cruz Biotechnology, Inc., Dallas, TX, USA), caspase 3 (1:2000; cat. no. sc-7148; Santa Cruz Biotechnology, Inc., Dallas, TX, USA), Bcl-2 (1:2000; cat. no. sc-7382; Santa Cruz Biotechnology, Inc., Dallas, TX, USA), caspase 8 (1:1000; cat. no. sc-5263; Santa Cruz Biotechnology, Inc., Dallas, TX, USA), DDAH1 (1:1000; cat. no. ab180599; Abcam, Cambridge, UK), p38 (1:1000; cat. no. ab119916; Abcam, Cambridge, UK), GAPDH (1:5000; cat. no. sc-32233; Santa Cruz Biotechnology, Inc., Dallas, TX, USA) were added and incubated overnight at 4°C. Then, the membrane was washed three times with PBST, and a horseradish peroxidase-labeled anti-mouse secondary antibody (1:4000; cat. no. ab6789; Abcam, Cambridge, UK), anti-rabbit secondary antibody (1:4000; cat. no.ab6721; Abcam, Cambridge, UK) and anti-rat secondary antibody(1:4000; cat. no. ab6734; Abcam, Cambridge, UK) were incubated for 1.5 h at room temperature. The film was washed three times. Proteins were visualized using a Clarity Western enhanced chemiluminescence Substrate (Bio-Rad Laboratories, Inc., Hercules, CA, USA) and a Tanon 5200 Full automatic chemiluminescence image analysis system (Tanon Science and Technology Co., Ltd, Shanghai, China).

Real-time PCR

RNA was extracted with Trizol reagent (Invitrogen, USA). Real-time PCR was performed using SYBR Premix Ex Taq (TaKaRa, Japan) and aMx3000P instrument (Sigma, USA). Gene expression was analyzed by Stratagene Mx3000P software. The primer sequence: NF-κB, F 5′-GGCAGACGA TGATCCCTACG-3′, R 5′-TGTTGACAGTG GTATTTCT GGTG-3′; TNF-α, F 5′-CCACCACGCTCTTCTGTCTA-3′, R 5′-GAGAGGGAGGCCATTTGGGA-3′; IL-1β, F 5′-CCTG TTCTTTGAAGTTGACGG-3′, R 5′-AGCTTCTCCA CAGC CACAAT-3′; IL-4, F 5′-CCATATCCACGGATGCGACA-3′, R 5′-CGTTGCTGTGAGGACGTTTG-3′; IL-6, F 5′-TACCA CTCCCAACAGACCTG-3′, R 5′-GGTACTCCAG AAGAC CAGAGG-3′; IL-10, F 5′-CACTGCTATGCTGCCTGCTCT-3′, R 5′-GAGTCGGTTAGCAGTATGTTGT-3′; MDA5, F 5′-AGTGTCTCCACTTGCTGACC-3′, R 5′-CAGCAGCTCT CTTACACCTGA-3′; IREα, F 5′-AGCACAGTTA CACTG CCTGAG-3′, R 5′-CTTCCACGTGTGTTGGGACCT-3′; SOD-1, F 5′-GAGCATTCCATCATTGGCCG-3′, R 5′-GGCA ATCCCAATCACACCAC-3′; Bax, F 5′-TCCACCA AGAA GCTGAGCGA-3′, R 5′-TTGAAGTTGCC ATCAGCA AA C A-3′; caspase 3, F 5′-ATGGGAGCAAGTCAGTGGAC-3′, R 5′-GTCCACATCCGTACCAGAGC-3′; Bcl-2, F 5′-TGAGT ACCTGAACCGGCATC-3′, R 5′-AAGCCCAGACTCATTC AACCA-3′; caspase 8, F 5′-CCTAGACTGCAAC CGAGA GG-3′, R 5′-TCCAACTCGCTCACTTCTTCTG-3′; DDAH1, F 5′-AGGTGCTGAAATCTTGGCTG-3′, R 5′-GCAGA TTC GCTGGACCCTAT-3′; p38, F 5′-TGACCCTTA TGACCA G TCCTTT-3′, R 5′-GTCAGGCTCTTCCACTCATCTAT-3′; G A PDH, F 5′-GGTCCCAGCTTAGGTTCATCA-3′, R 5′-CC GTTCACACCGACCTTCA-3′.

Immunofluorescence staining

The lung tissue was dewaxed with xylene, an ethanol gradient, 0.1% TritonX-100 for 30 min, and washed three times with PBS for 5 min. Then, 10% sheep serum were incubated for 30 min, incubated with the primary antibody at 4°C in a wet box overnight, then fluorescent secondary antibody staining, microscopic observation and photography.

ROS detection

The lung tissue was frozen in PBS for 5 min twice and dihydroethidium (DHE) was incubated for 10 min in the dark for 10 min. Then samples were immersed in PBS for 5 min twice and observed under a fluorescence microscope.

TUNEL staining

The change in apoptotic cells in each mouse tissue was detected by a TUNEL kit (Cloud-Clone Corp, USA). The procedure was carried out according to the manufacturer's instructions. The apoptotic cell nuclei were stained brown. Five different visual fields were randomly selected at high magnification (×400) to calculate the apoptotic index.

Statistical analysis

SPSS 20.0 software was used for statistical analysis. Measurement data were evaluated by *t*-test and analysis of variance. The data indicate the mean ± standard deviation, and all statistical tests were bilateral probabilistic tests. The inspection level is a = 0.05.

Results

The thickness of aluminum film is proportional to the burst strength

Different thicknesses of aluminum film were used to control the shock wave peak overpressure value, while the same layer thickness of aluminum produced a shock wave waveform that was very similar. Aluminum film thickness was associated with overpressure: 0.8 mm produced 95.85 ± 15.61 PSI peak overpressure (Supplementary Figure A), 1.0 mm produced 121.81 ± 14.63 PSI peak overpressure (Supplementary Figure B), 1.2 mm produced 187.70 ± 20.86 PSI peak overpressure (Supplementary Figure C), 1.4 mm produced 337.46 ± 18.30 PSI peak overpressure (Supplementary Figure 2(d)), and 1.6 mm produced 423.32 ± 11.64 PSI peak overpressure (Supplementary Figure E). Aluminum film thickness was positively correlated with peak overpressure (R^2=0.94) (Figure 2). The ranges of peak pressures could be from 95.85 ± 15.61 PSI to 423.32 ± 11.64 PSI.

The number of aluminum layers is proportional to mortality rate

Increasing aluminum film thickness increased the mortality of mice with a positive correlation linear relationship (R^2=0.92) (Figure 3(a)) according to the pressure and mortality values. A follow-up lung injury experiment using an aluminum film thickness of 1.4 mm showed a pressure of 337.46 ± 18.30 PSI induced a mortality rate of approximately 23.2%.

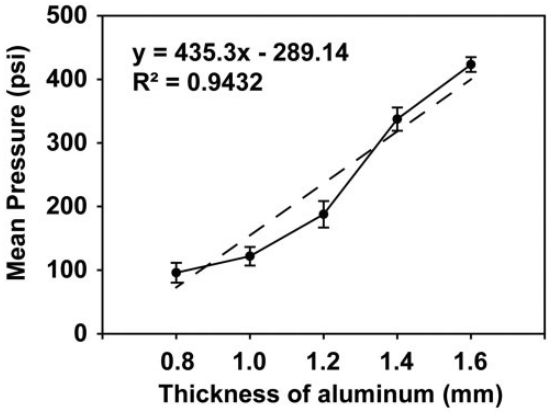

Figure 2. The shock wave waveform and overpressure value are proportional to the aluminum layer thickness. The overpressure value increases with increasing aluminum thickness.

Pulmonary blast injury causes mouse heart rate and blood pressure disorders

After the blast, mice in each group were incapacitated with a slow breathing rate and mild epilepsy. After 1 h of slow recovery from anesthesia, the mice were weak, slow, and had a loss of appetite. Compared with the control group, the heart rate of the experimental mice was significantly decreased ($P < 0.05$) within 3–12 h, returned to normal at 24–48 h, was significantly increased at 7 days ($P < 0.05$), and returned to normal at 14 days (Figure 3(b)). Compared with the control group, the blood pressure was significantly decreased ($P < 0.05$) at 3–12 h, then returned to normal (Figure 3(c)).

Pulmonary injury is caused by LBI

Compared with the control group, the wet/dry weight of lungs was significantly higher in the 6 h, 12 h and 24 h groups ($P < 0.05$), and returned to normal at 24 h (Figure 3 (d)). Pulmonary edema after 12 h was observed. Mice in the control group had intact lung tissue with no obvious bleeding. In the 3-h group, a large number of diffuse bleeding-spots gradually increased with time. During the 12–48-h period, the most serious mass (Figure 4(a)) HE staining showed that alveolar cavities were fused with bullae like changes, inflammatory cell infiltration, and alveolar wall thickening (Figure 4(b)). According to the lung injury score, there was obvious lung injury ($P < 0.05$) at 3 h and the injury increased with time and reached a peak at 12 h ($P < 0.05$), then gradually recovered at 7 days compared with the control group (Figure 4(c)). The Evans blue test showed pulmonary vascular breakdown after pulmonary blast injury, and pulmonary vascular rupture led to the leakage of Evans blue dye into the lung tissue. The degree of diffuse vascular leakage reached a peak at 24 h ($P < 0.05$), followed by a gradual decrease in injury and recovery at seven days (Figure 4(c) and (d)).

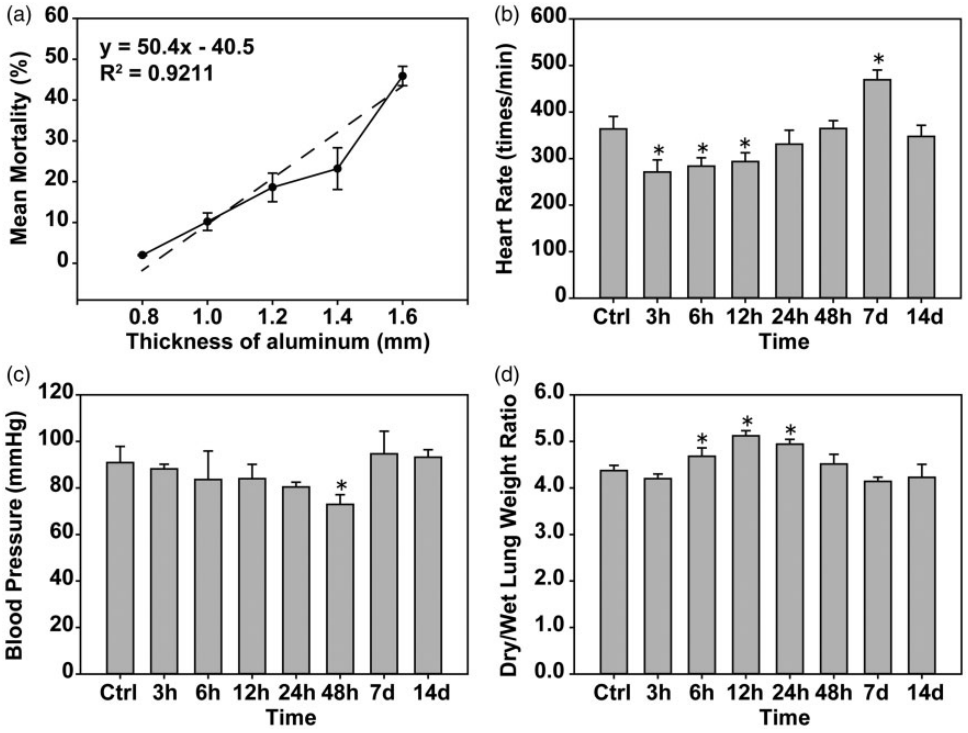

Figure 3. The aluminum layer membrane is proportional to the mortality rate, pulmonary blast injury and mouse heart rate, blood pressure disorders, and pulmonary edema. (a) A positive correlation between the mortality of mice and aluminum film thickness was observed. (b and c) The effects of pulmonary blast injury on heart rate and blood pressure were detected in mice. (d) The wet and dry weights of lung tissues were measured, and the change in their ratio was compared. $^*P < 0.05$, compared with the control group, $n = 5$.

Inflammation of lung tissue is induced by pulmonary blast injury

Western blot and real-time PCR showed the expression of NF-κB in the 3-h group was decreased with time compared with the control group. TNF-α and IL-1β in the 3 and 6-h groups were unchanged compared with the control group and IL-6 in the 6-h group was significantly higher than in the control group ($P < 0.05$) (Figure 5(a) to (f)). Immunofluorescence was used to detect NF-κB in the lung tissue and showed similar results to the Western blotting and real-time PCR (Figure 5(g)).

Oxidative stress response is induced by LBI in lung tissues of mice

Western blot and real-time PCR were used to detect oxidative stress-related factors in lung tissues. Compared with the control group, the expression of SOD-1 was decreased and the expression of MDA5 and IREα was increased in the 6-h group, reaching the peak, followed by a decrease in the expression (Figure 6(a) to (d)). Detection of ROS in the lung tissues revealed that the blastocyst injury significantly increased ROS expression over time, which reached a peak at 24 h and then gradually recovered (Figure 6(e)).

Apoptosis of mouse lung tissue is induced by LBI

Western blot and real-time PCR were used to detect apoptosis-related factors in lung tissues. Compared with the control group, the expression of Bcl-2 decreased gradually with the blast time, reached a peak at 24 h, and then returned to normal. Bax was normal at 12–48 h. The expression of caspase 3 increased gradually with blast time, reached a peak at 24 h, and then gradually returned to normal (Figure 7(a) to (d)). TUNEL results showed that pulmonary blast injury induced lung injury that increased with time until it reached a peak at 24 h and gradually returned to normal (Figure 7(e)).

Discussion

The study of lung injury caused by blast injury is a focus of global research on blast injury, but its detailed damage process and molecular mechanisms are not clear. In this study, an accurate model of pulmonary blast injury in mice was developed. The damage and molecular changes in lung tissue were studied at different time points after successful blasts. The results showed mouse heart rate and blood pressure disorders, significant edema of lung tissues, vascular rupture, pulmonary tissue diffuse bleeding at 3 h after pulmonary blast injury, and that the lung injury gradually increased between 12 to 24 h post damage, which then returned to normal. Previous studies reported that shock waves induced rat and mouse alveolar and pulmonary capillary injury, pulmonary hemorrhage, and pulmonary edema.[17–19] Clinical studies have shown that the initial signs of LBI are cough, hemoptysis, and other pulmonary symptoms. Some of them have hemothorax and/or combined pneumothorax. The majority of patients have lung infections with high mortality. The main cause of death is shock, respiratory failure, or septicemia.[20,21]

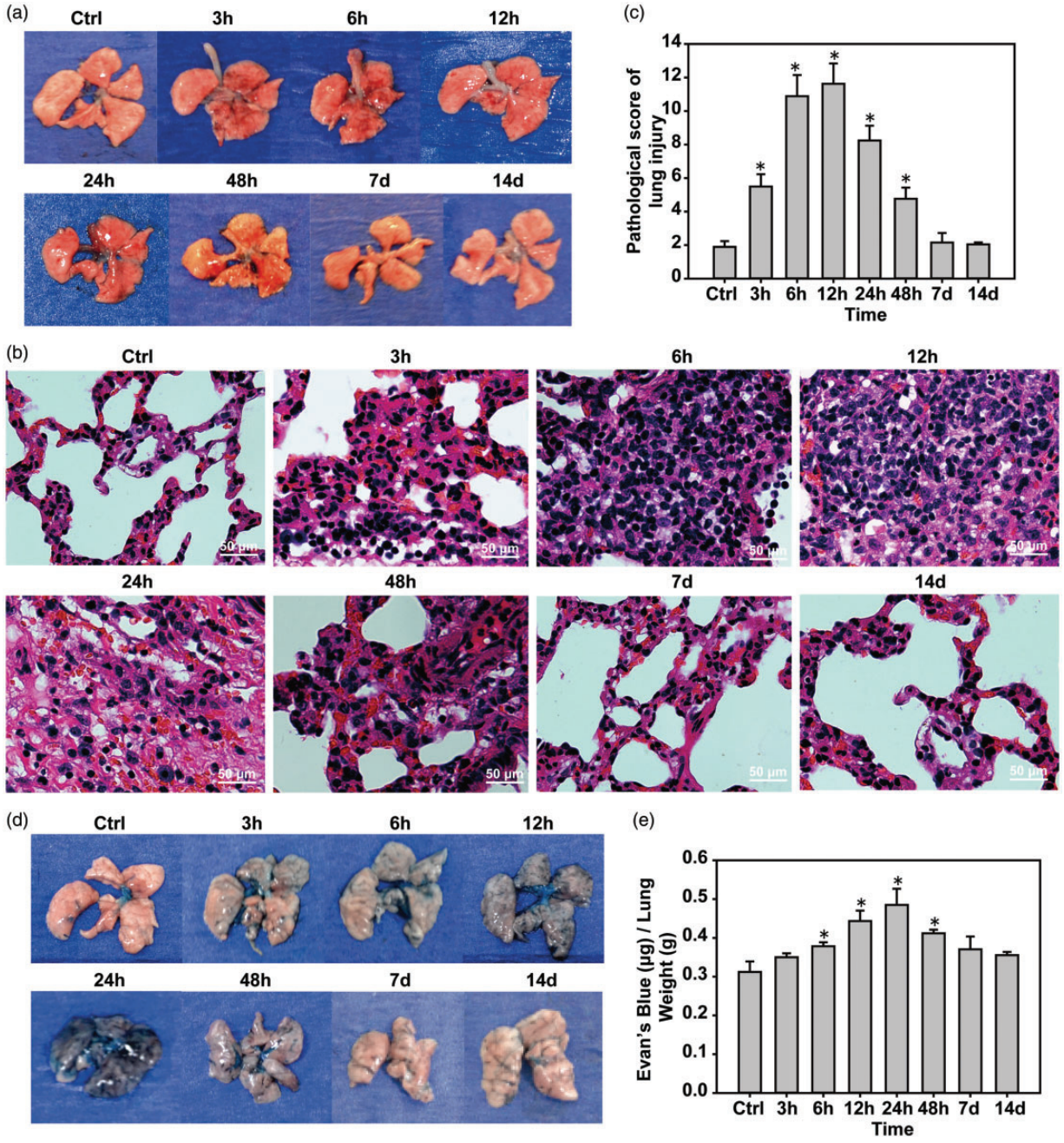

Figure 4. Pulmonary blast injury causes mouse lung vascular rupture and lung injury. (a) Pulmonary blast injury of mouse lungs caused diffuse pulmonary hemorrhage. (b and c) Lung tissue HE staining and lung injury scores. (d and e) Evans blue test to detect pulmonary vascular injury. *$P < 0.05$, compared with the control group, $n = 5$. (A color version of this figure is available in the online journal.)

This study found that blast injury increased the number of inflammatory cells in the lung tissue, and induced alveolar fusion into the lung cavity and alveolar wall thickening, which were visible after the start of the blast injury and increased with an increase in damage until a peak at 24 h post blast, and then gradually decreased. The expression of NF-κB, TNF-α, IL-1β, IL-6, and IL-10 was detected by Western blot, real-time PCR, and immunofluorescence assay. The results showed the different expression of inflammatory factors ($P < 0.05$). However, the expression of NF-κB reached a peak at 3 h, and the expressions of TNF-α, IL-1β and IL-6 reached a peak at 12 h. The anti-inflammatory cytokine IL-10 began to decrease at 6 h after pulmonary blast injury, reached a trough at 12 h, and then gradually increased. Monocyte chemoattractant protein-1 (MCP-1) and cytokine-induced neutrophil chemokine-1 (CINC-1) mRNA was high expression in the lungs of the rats treated with 140 kPa (20.31 PSI) at 2 d, and all inflammatory mediators returned to normal at 8 d.[22] Another study found that rats exposed to 120 kPa (17.40 PSI) overpressure induced myeloperoxidase, CINC-1, ICAM-1, and iNOS activation, as well as diffuse bleeding inflammation at 48 h and that inflammatory symptoms had disappeared by 192 h.[23] Although this study found that

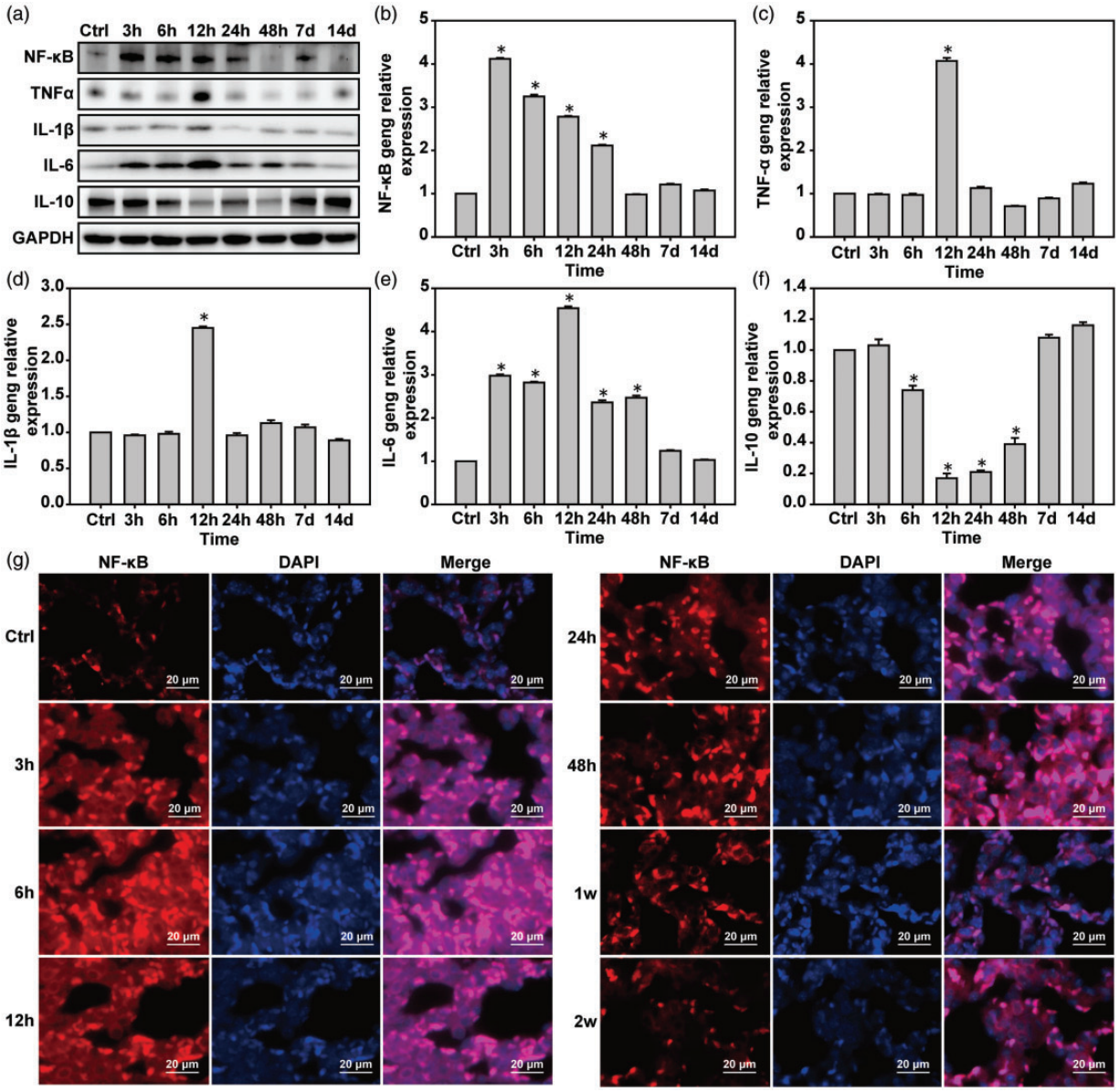

Figure 5. Pulmonary blast injury induces pulmonary inflammatory responses. (a) Western blot was used to detect the expressions of NF-κB, TNF-α, IL-1β, and IL-6. (b–f) Real-time PCR was used to detect the expressions of NF-κB, TNF-α, IL-1β, and IL-6 mRNA. (g) Immunofluorescence was used to detect the expression of NF-κB protein. *$P < 0.05$, compared with the control group, $n = 5$. (A color version of this figure is available in the online journal.)

pulmonary blast injury caused pulmonary inflammatory responses, the activation time of the inflammatory response with the shock wave overpressure and experimental animal species varied. Pulmonary contusion and pulmonary blast injury pathogenesis were induced by a high pressure wave on the chest, which increased the intrathoracic pressure, oppression of the lungs, pulmonary hemorrhage and edema, when the external force to eliminate the deformation of the thoracic bounced back in the chest. Pressure can lead to additional damage to the original injury area and pathological changes in alveoli and capillaries.[24–28] Pulmonary contusion studies have shown that 2–3 h after mouse lung contusion IL-6, TNF-α expression increased, IL-10 expression decreased, and inflammatory responses were activated.[29–31] In a clinical study of military personnel exposed to explosions, blood samples from 62 military personnel were tested for acute peripheral blood cytokine levels and the results showed that moderate shocks could result in significant increases in IL6 and TNF-α concentrations.[32] In summary, the shock waves caused by lung injury in mice induces early inflammatory responses, but if the subject does not succumb they will gradually recover over time.

This study found that pulmonary blast injury activated oxidative stress in lung tissues. The results of ROS staining showed that the oxidative stress response after LBI was gradually activated, reached a peak at 24 h, then gradually recovered. The expression of MDA-5 and IREα was induced by pulmonary blast injury, and the expression of SOD-1 was inhibited. MDA5 reached a peak at 12 h, IREα reached a peak at 24 h, and SOD-1 reached a trough at 48 h post blast. Oxidative stress induced by LBI was most

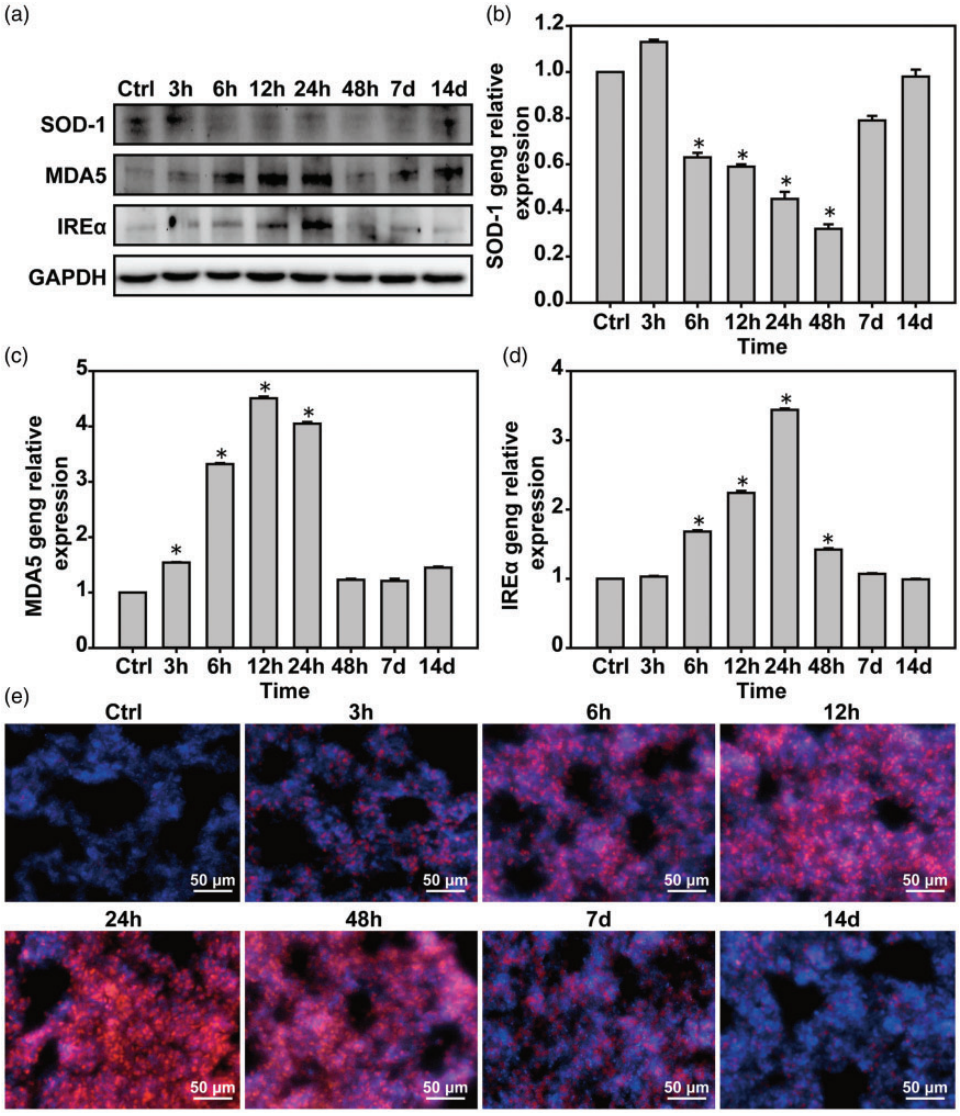

Figure 6. Lung blast injury induces lung tissue oxidative stress. (a) Western blot was used to detect the expressions of SOD-1, MDA5, and IREα proteins. (b–d) Real-time PCR was used to detect the expressions of SOD-1, MDA5, and IREα mRNA. (e) Dihydrodepine to detect lung tissue ROS. *$P < 0.05$, compared with the control group, $n = 5$. (A color version of this figure is available in the online journal.)

severe at 24 h and slightly slower than the activation of the inflammatory response. Studies of rats exposed to 120 kPa (17.40 PSI) overpressure showed, oxidative stress was induced at 24–48 h, that myeloperoxidase (MPO), heme oxygenase-1 (HO-1), antioxidant enzyme and manganese superoxide dismutase (MnSOD) expressions were induced, protein oxidation and nitrification were increased, and the symptoms were recovered at 192 h after exposure.[23] Lavery *et al.*[33] showed that the blast injury can be an indirect physiological disease that causes bradycardia, hypotension, tissue hypoxia, and oxidative stress. Other studies have shown that the blast injury induced free radical-mediated oxidative stress in the lungs as well as antioxidant depletion, lipid peroxidation, and hemoglobin (Hb) oxidation.[34] Liener *et al.*[35] showed that MPO activity reached peak values at 6 h and 72 h after pulmonary contusion in rats. The results of the above studies show that lung injury induces the activation of oxidative stress in lung tissues.

This study found that the pulmonary blast injury induced lung tissue apoptosis which was most marked at 12–48 h post blast, and was based on the expressions of Bax and caspase 3 that increased the inhibition of apoptosis factor Bcl-2 expression. All reached a peak at 24 h.[35] Liener *et al.* showed that the number of apoptotic cells in lung tissue was highest at 48 h after pulmonary contusion and that the expression of caspase 8 was increased by 39%. Other studies showed that the pulmonary contusions induced the expression of caspase-3 and Bax[36,37] and that the pulmonary contusion induced rat type II alveolar epithelial cell apoptosis, which reached a peak at 48 h, while no difference was seen for FasL, Fas, caspase 8 and caspase 3, Bax and Bcl-2.[38] Our results confirm those of previous studies and show that the impaired lung injury induces apoptosis.

In conclusion, pulmonary blast injury induced early inflammatory responses, oxidative stress responses, and

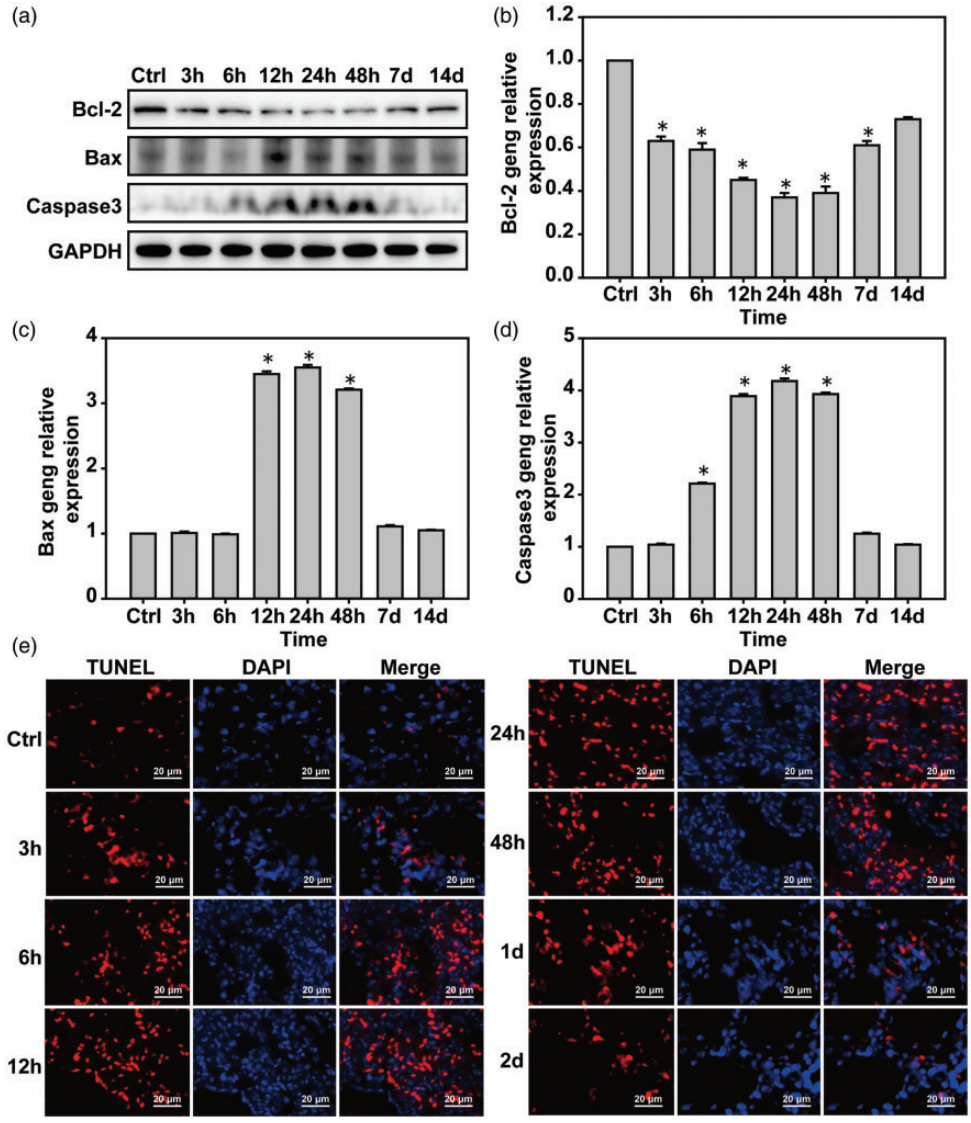

Figure 7. Lung blast injury induces lung tissue cell apoptosis. (a) Western blot was used to detect the expressions of Bcl-2, Bax, and caspase 3 proteins. (b–d) Real-time PCR was used to detect the expressions of Bcl-2, Bax, and caspase 3 mRNA. (e) TUNEL detection of lung tissue apoptosis. *$P < 0.05$, compared with the control group. *$P < 0.05$, compared with the control group, $n = 5$. (A color version of this figure is available in the online journal.)

apoptosis. We developed a pulmonary blasting simulation device to investigate mouse LBI. The resulting lung injury was the same as the lung injury caused by existing pulmonary blasting simulation devices. However, compared with conventional devices, it has the advantages of simple operation, controlled process, high repetition rate controlling the shock wave acting on the chest only. Our results found that the impact of different overpressure shock waves caused different degrees of injury, inflammation, oxidative stress, and apoptosis over time. The greater the lung tissue inflammatory response, oxidative stress response and activation of early apoptosis, the more serious the consequences to the subject.

Authors' contributions: Changci Tong, Yunen Liu and Mingxiao Hou participated in the design of this study. Changci Tong, Yubiao Zhang, Peifang Cong, Xiuyun Shi, Lin Shi and Ying Liu carried out the study, collected important background information and data acquisition. Yunen Liu, Yubiao Zhang and Hongxu Jin participated in the design of the simulation device of explosive knocking. Changci Tong carried out data analysis and statistical analysis and drafted the manuscript. All authors read and approved the final manuscript.

DECLARATION OF CONFLICTING INTERESTS

The author(s) declared no potential conflicts of interest with respect to the research, authorship, and/or publication of this article.

FUNDING

The author(s) disclosed receipt of the following financial support for the research, authorship, and/or publication of this article: This work was supported by the 2012 PLA foundation of China during the Twelfth Five-year Plan Period [CSY12J002], and 2013 PLA foundation of China during the

Twelfth Five-year Plan Period [CSY13J003]. We thank J. Ludovic Croxford, PhD, from Liwen Bianji, Edanz Group China (www.liwenbianji.cn/ac), for editing the English text of a draft of this manuscript.

REFERENCE

1. Born CT. Blast trauma: the fourth weapon of mass destruction. *Scand J Surg* 2005;**94**:279–85
2. Zhao Y, Zhou YG. The past and present of blast injury research in China. *Chin J Traumatol* 2015;**18**:194–200
3. Wolf SJ, Bebarta VS, Bonnett CJ, Pons PT, Cantrill SV. Blast injuries. *Lancet* 2009;**374**:405–15
4. Risdall JE, Menon DK. Traumatic brain injury. *Philos Trans R Soc Lond B Biol Sci* 2011;**366**:241–50
5. Kabu S, Jaffer H, Petro M, Dudzinski D, Stewart D, Courtney A, Courtney M, Labhasetwar V. Blast-associated shock waves result in increased brain vascular leakage and elevated ROS levels in a rat model of traumatic brain injury. *PLoS One* 2015;**10**:e0127971
6. Buhrer S, Tilney P. Blast lung injury in a 20-year-old man after a home explosion. *Air Med J* 2012;**31**:10–2
7. Mishra SK, Kumar BS, Khushu S, Singh AK, Gangenahalli G. Early monitoring and quantitative evaluation of macrophage infiltration after experimental traumatic brain injury: a magnetic resonance imaging and flow cytometric analysis. *Mol Cell Neurosci* 2017;**78**:25–34
8. DeMar J, Sharrow K, Hill M, Berman J, Oliver T, Long J. Effects of primary blast overpressure on retina and optic tract in rats. *Front Neurol* 2016;**7**:59
9. Samra T, Pawar M, Kaur J. Challenges in management of blast injuries in intensive care unit: case series and review. *Ind J Crit Care Med* 2014;**18**:814–8
10. Goodrich JA, Kim JH, Situ R, Taylor W, Westmoreland T, Du F, Parks S, Ling G, Hwang JY, Rapuano A, Bandak FA, de Lanerolle NC. Neuronal and glial changes in the brain resulting from explosive blast in an experimental model. *Acta Neuropathol Commun* 2016;**4**:124
11. Kawoos U, Gu M, Lankasky J, McCarron RM, Chavko M. Effects of exposure to blast overpressure on intracranial pressure and blood-brain barrier permeability in a rat model. *PLoS One* 2016;**11**:e0167510
12. Kuriakose M, Skotak M, Misistia A, Kahali S, Sundaramurthy A, Chandra N. Tailoring the blast exposure conditions in the shock tube for generating pure, primary shock waves: the end plate facilitates elimination of secondary loading of the specimen. *PLoS One* 2016;**11**:e0161597
13. Mishra V, Skotak M, Schuetz H, Heller A, Haorah J, Chandra N. Primary blast causes mild, moderate, severe and lethal TBI with increasing blast overpressures: experimental rat injury model. *Sci Rep* 2016;**6**:26992
14. Perez-Garcia G, Gama Sosa MA, De Gasperi R, Lashof-Sullivan M, Maudlin-Jeronimo E, Stone JR, H, F, Ahlers ST, Elder GA. Chronic post-traumatic stress disorder-related traits in a rat model of low-level blast exposure. *Behav Brain Res* 2018;**340**:117–25
15. Rostami E. Traumatic brain injury models in animals. *Methods Mol Bio*2016;**1462**:47–59
16. Awwad HO, Gonzalez LP, Tompkins P, Lerner M, Brackett DJ, Awasthi V, Standifer KM. Blast overpressure waves induce transient anxiety and regional changes in cerebral glucose metabolism and delayed hyperarousal in rats. *Front Neurol* 2015;**6**:132
17. Rotta AT, Gunnarsson B, Hernan LJ, Fuhrman BP, Steinhorn DM. Partial liquid ventilation influences pulmonary histopathology in an animal model of acute lung injury. *J Crit Care* 1999;**14**:84–92
18. Elsayed NM, Gorbunov NV. Pulmonary biochemical and histological alterations after repeated low-level blast overpressure exposures. *Toxicol Sci* 2007;**95**:289–96
19. Chavko M, Prusaczyk WK, McCarron RM. Protection against blast-induced mortality in rats by hemin. *J Trauma* 2008;**65**:1140–5; discussion 5
20. Zhang Y, Meng WZ, Wang MJ, Ren WJ, Wang GZ, Zhang GB. Zhu, MS. The epidemiological features of blast injury of lungs caused by gas explosion. *Zhonghua Lao Dong Wei Sheng Zhi Ye Bing Za Zhi* 2012;**30**:582–3
21. Lee K, Yoon J, Min K, Lee J, Kang S, Hong SJ, Yoon SH, Lee JS, Nam KW, Cho SH, Park H, Young KI. An objective index to estimate the survival rate of primary blast lung injury. *Conf Proc IEEE Eng Med Biol Soc* 2014;**2014**:1206–9
22. Perl M, Hohmann C, Denk S, Kellermann P, Lu D, Braumuller S, Bachem MG, Thomas J, Knoferl MW, Ayala A, Gebhard F, Huber-Lang MS. Role of activated neutrophils in chest trauma-induced septic acute lung injury. *Shock* 2012;**38**:98–106
23. Chavko M, Prusaczyk WK, McCarron RM. Lung injury and recovery after exposure to blast overpressure. *J Trauma* 2006;**61**:933–42
24. Ritenour AE, Baskin TW. Primary blast injury: update on diagnosis and treatment. *Crit Care Med* 2008;**36**:S311–7
25. Cohn SM, Dubose JJ. Pulmonary contusion: an update on recent advances in clinical management. *World J Surg* 2010;**34**:1959–70
26. Satoh Y, Sato S, Saitoh D, Tokuno S, Hatano B, Shimokawaji T, Kobayashi H, Takishima K. Pulmonary blast injury in mice: a novel model for studying blast injury in the laboratory using laser-induced stress waves. *Lasers Surg Med* 2010;**42**:313–8
27. Peng LH, Guo GH. Advances in the research of blast lung injury. *Zhonghua Shao Shang Za Zhi* 2016;**32**:156–9
28. Scott TE, Kirkman E, Haque M, Gibb IE, Mahoney P, Hardman JG. Handling editor PSMPrimary blast lung injury – a review. *Br J Anaesth*2017;**118**:311–6
29. Knoferl MW, Liener UC, Seitz DH, Perl M, Bruckner UB, Kinzl L, Gebhard F. Cardiopulmonary, histological, and inflammatory alterations after lung contusion in a novel mouse model of blunt chest trauma. *Shock* 2003;**19**:519–25
30. Perl M, Gebhard F, Braumuller S, Tauchmann B, Bruckner UB, Kinzl L, Knoferl MW. The pulmonary and hepatic immune microenvironment and its contribution to the early systemic inflammation following blunt chest trauma. *Crit Care Med* 2006;**34**:1152–9
31. Niesler U, Palmer A, Froba JS, Braumuller ST, Zhou S, Gebhard F, Knoferl MW, Seitz DH. Role of alveolar macrophages in the regulation of local and systemic inflammation after lung contusion. *J Trauma Acute Care Surg* 2014;**76**:386–93
32. Gill J, Motamedi V, Osier N, Dell K, Arcurio L, Carr W, Walker P, Ahlers S, LoPresti M, Yarnell A. Moderate blast exposure results in increased IL-6 and TNFalpha in peripheral blood. *Brain Behav Immunity* 2017;**65**:90–4
33. Lavery GG, Lowry KG. Management of blast injuries and shock lung. *Curr Opin Anaesthesiol* 2004;**17**:151–7
34. Elsayed NM, Armstrong KL, William MT, Cooper MF. Antioxidant loading reduces oxidative stress induced by high-energy impulse noise (blast) exposure. *Toxicology* 2000;**155**:91–9
35. Liener UC, Knoferl MW, Strater J, Barth TF, Pauser EM, Nussler AK, Kinzl L, Bruckner UB, Gebhard F. Induction of apoptosis following blunt chest trauma. *Shock* 2003;**20**:511–6
36. Wagner F, Scheuerle A, Weber S, Stahl B, McCook O, Knoferl MW, Huber-Lang M, Seitz DH, Thomas J, Asfar P, Szabo C, Moller P, Gebhard F, Georgieff M, Calzia E, Radermacher P, Wagner K. Cardiopulmonary, histologic, and inflammatory effects of intravenous Na2S after blunt chest trauma-induced lung contusion in mice. *J Trauma* 2011;**71**:1659–67
37. Hafner S, Wagner K, Wepler M, Matallo J, Groger M, McCook O, Scheuerle A, Huber-Lang M, Frick M, Weber S, Stahl B, Jung B, Calzia E, Georgieff M, Moller P, Dietl P, Radermacher P, Wagner F. Physiological and immune-biological characterization of a long-term murine model of blunt chest trauma. *Shock* 2015;**43**:140–7
38. Seitz DH, Perl M, Mangold S, Neddermann A, Braumuller ST, Zhou S, Bachem MG, Huber-Lang MS, Knoferl MW. Pulmonary contusion induces alveolar type 2 epithelial cell apoptosis: role of alveolar macrophages and neutrophils. *Shock* 2008;**30**:537–44

(Received February 21, 2018, Accepted May 21, 2018)